Efficient Use of Energy in Thermal Systems

N. Allouache, S. Chikh

Abstract—**Energy conservation is one of the major concerns in the modern high tech era due to the limited amount of energy resources and the increasing cost of energy. Predicting an efficient use of energy in thermal systems like heat exchangers can only be achieved if the second law of thermodynamics is accounted for. The performance of heat exchangers can be substantially improved by many passive heat transfer augmentation techniques. These latters permit to improve heat transfer rate and to increase exchange surface, but on the other side, they also increase the friction factor associated with the flow. This raises the question of how to employ these passive techniques in order to minimize the useful energy. The objective of this present study is to use a porous substrate attached to the walls as a passive enhancement technique in heat exchangers and to find the compromise between the hydrodynamic and thermal performances under turbulent flow conditions, by using a second law approach. A modified k- ε model is used to simulate the turbulent flow in the porous medium and the turbulent shear flow is accounted for in the entropy generation equation. A numerical modeling, based on the finite volume method is employed for discretizing the governing equations. Effects of several parameters are investigated such as the porous substrate properties and the flow conditions. Results show that under certain conditions of the porous layer thickness, its permeability and its effective thermal conductivity the minimum rate of entropy production is obtained.**

Index Terms—**Energy conservation, Heat exchanger, second law approach, numerical modeling**

I. INTRODUCTION

The depleting energy resources and increasing energy costs call for more effective use of available energy. Heat transfer and the design of heat transfer equipment continue to be an important issue in energy conservation. Therefore, developing and improving heat exchanger effectiveness have been the main attempts of many studies. Developing and improving heat exchanger effectiveness have been the main attempts of many studies. Owing to the fact that enhancement techniques are always achieved at the expense of fluid friction losses, an optimal trade-off has become the critical challenge for the design work. The optimal design can be achieved through the efficient use of energy and if the second law of thermodynamic is accounted for.

The use of porous medium as a passive augmentation technique increases exchange surface and improves heat transfer rate, but generates a high pressure drop. In order to find the compromise between hydrodynamics and thermal performances, a second law approach, based on the entropy generation seems very suited. Yet only few numbers of studies considered entropy generation in convection heat transfer with porous media. The majority of these studies are presented for laminar flows [1-3]. Until now, the study of second law in turbulent flow with a porous media is almost nonexistent.

The present work mainly investigates the entropy generation and the irreversibilities due to the turbulent flow in porous annular heat exchanger (Fig. 1) and to find the optimal conditions that allow to reduce pressure drop, to enhance heat transfer and to minimize energy losses. The mathematical model based on the modified κ-ε model and turbulent entropy generation equation is developed and solved by using the finite volume method.
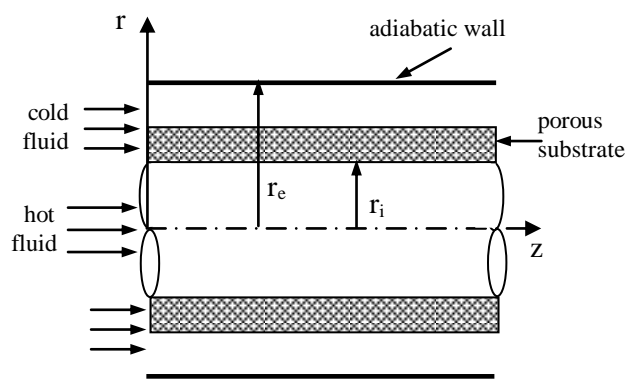

Fig. 1. Schematic of physical domain

II. MATHEMATICAL MODEL

The fluid is assumed to be incompressible and the flow two-dimensional and axisymmetric. The porous substrate is considered homogeneous, isotropic and saturated with a single-phase. The fluid is in local thermal equilibrium with the solid matrix.

The average continuity, momentum, energy, and local entropy generation equations in cylindrical coordinates are [4-7]:

N. Allouache is with the Department of Mechanical and Process Engineering, University of Science and Technology Houari Boumedien, B.P 32 El Alia, Algeria (corresponding author to provide phone: +213-773-661916; e-mail: allouache_nadia@yahoo.fr).

S. Chikh is with the Department of Mechanical and Process Engineering, University of Science and Technology Houari Boumedien, B.P 32 El Alia, Algeria (e-mail: salahschikh@yahoo.fr).

Continuity equation:

$$\frac{\partial U}{\partial z} + \frac{1}{r}\frac{\partial (rV)}{\partial r} = 0 \tag{1}$$

Momentum equation in axial direction:

$$U\frac{\partial U}{\partial z} + \frac{V}{r}\frac{\partial (rU)}{\partial r} = -\frac{1}{\rho_f}\frac{\partial P}{\partial z} + \frac{\partial}{\partial z}\left((\nu_t + \nu J)\frac{\partial U}{\partial z}\right)$$
$$+ \frac{1}{r}\frac{\partial}{\partial r}\left((\nu_t + \nu J)r\frac{\partial U}{\partial r}\right) - \frac{2}{3}\frac{\partial k}{\partial z} + \frac{\partial}{\partial z}\left(\nu_t\frac{\partial U}{\partial z}\right)$$
$$+ \frac{1}{r}\frac{\partial}{\partial r}\left(\nu_t r\frac{\partial V}{\partial z}\right) - \phi\frac{\nu}{K}U - \phi^2\frac{c_F}{K^{1/2}} \tag{2}$$
$$\left(|U|U + \frac{1}{|U|}\left(\frac{2}{3}kU - \nu_t\left(2U\frac{\partial U}{\partial z} + V\left(\frac{\partial U}{\partial r} + \frac{\partial V}{\partial z}\right)\right)\right)\right)$$

Momentum equation in radial direction:

$$U\frac{\partial V}{\partial z} + \frac{V}{r}\frac{\partial (rV)}{\partial r} = -\frac{1}{\rho_f}\frac{\partial P}{\partial z} + \frac{\partial}{\partial z}\left((\nu_t + \nu J)\frac{\partial V}{\partial z}\right)$$
$$+ \frac{1}{r}\frac{\partial}{\partial r}\left((\nu_t + \nu J)r\frac{\partial V}{\partial r}\right) - \frac{2}{3}\frac{\partial k}{\partial z} + \frac{\partial}{\partial z}\left(\nu_t\frac{\partial V}{\partial r}\right)$$
$$+ \frac{1}{r}\frac{\partial}{\partial r}\left(\nu_t r\frac{\partial V}{\partial r}\right) - \frac{2\nu_t V}{r^2} - \phi\frac{\nu}{K}V - \phi^2\frac{c_F}{K^{1/2}} \tag{3}$$
$$\left(|U|V + \frac{1}{|U|}\left(\frac{2}{3}kV - \nu_t\left(2V\frac{\partial V}{\partial r} + V\left(\frac{\partial V}{\partial z} + \frac{\partial U}{\partial r}\right)\right)\right)\right)$$

U, V are the time-averaged fluid velocities, $\nu_t = C_\mu k^2/\varepsilon$ is the eddy viscosity, ϕ is the porosity, K is the porous medium permeability and $J = \mu_e/\mu_f$ is the viscosity ratio.

Energy equation:

$$U\frac{\partial \overline{T}}{\partial z} + \frac{V}{r}\frac{\partial (r\overline{T})}{\partial r} = \frac{\partial}{\partial z}\left(\left(\frac{R_c \nu}{\phi \, \mathrm{Pr}} + \frac{\nu_t}{\sigma_t}\right)\frac{\partial \overline{T}}{\partial z}\right)$$
$$+ \frac{1}{r}\frac{\partial}{\partial r}\left(\left(\frac{R_c \nu}{\phi \, \mathrm{Pr}} + \frac{\nu_t}{\sigma_t}\right)r\frac{\partial \overline{T}}{\partial r}\right) \tag{4}$$

$\overline{T}$ is the average temperature, Pr is the Prandtl number and $R_c = \lambda_e/\lambda_f$ is the thermal conductivity ratio.

Local rate of entropy generation equation:

The local rate of entropy generation in incompressible turbulent shear flows for Newtonian fluids is:

$$\dot{S}_g = \frac{\lambda_j}{\overline{T}^2}\left[\left(\frac{\partial \overline{T}}{\partial z}\right)^2 + \left(\frac{\partial \overline{T}}{\partial r}\right)^2\right]\left(1 + \frac{C_p \mu_t}{\sigma_t \lambda_j}\right) + \frac{\rho\varepsilon}{\overline{T}}$$
$$+ \frac{\mu_j}{\overline{T}}\left\{2\left[\left(\frac{\partial V}{\partial r}\right)^2 + \left(\frac{V}{r}\right)^2 + \left(\frac{\partial U}{\partial z}\right)^2\right] + \left(\frac{\partial U}{\partial r} + \frac{\partial V}{\partial z}\right)^2\right\} \tag{5}$$

The rate of entropy generation over the cross section is calculated by integration:

$$S_g = \int_{r_i}^{r_e} \dot{S}_g \, 2\pi r \, dr \tag{6}$$

The subscript j in λ_j and μ_j stands for h in the hot side and for c in the cold side, while in the porous region, j indicates the effective thermal conductivity in λ_j.

The model equations used for the turbulent kinetic energy and dissipation rate are:

Model equation for turbulent kinetic energy (k)

$$U\frac{\partial k}{\partial z} + \frac{V}{r}\frac{\partial (rk)}{\partial r} = P_k + \frac{\partial}{\partial z}\left(\left(\nu J + \frac{\nu_t}{\sigma_k}\right)\frac{\partial k}{\partial z}\right)$$
$$+ \frac{1}{r}\frac{\partial}{\partial r}\left(\left(\nu J + \frac{\nu_t}{\sigma_k}\right)r\frac{\partial k}{\partial r}\right) - J\varepsilon - G_k \tag{7}$$

where

$$P_k = \nu_t\left[2\left(\frac{\partial V}{\partial r}\right)^2 + 2\left(\frac{\partial U}{\partial z}\right)^2 + \left(\frac{\partial V}{\partial z} + \frac{\partial U}{\partial r}\right)^2 + 2\left(\frac{V}{r}\right)^2\right] \tag{8}$$

$$G_k = 2\phi\frac{\nu}{K}k + \frac{\phi^2 c_F}{K^{1/2}|U|}\left(-\frac{4}{3}C_s\frac{k^2}{\varepsilon}\left(\frac{5}{3}\left(U\frac{\partial k}{\partial z} + V\frac{\partial k}{\partial r}\right)\right.\right.$$
$$-\left(2U\frac{\partial}{\partial z}\left(\nu_t\frac{\partial U}{\partial z}\right) + 2\frac{V}{r}\frac{\partial}{\partial r}\left(\nu_t r\frac{\partial V}{\partial r}\right) - \frac{2\nu_t V}{r^2}\right)$$
$$+V\frac{\partial}{\partial z}\nu_t\left(\frac{\partial U}{\partial r} + \frac{\partial V}{\partial z}\right) + \frac{U}{r}\frac{\partial}{\partial r}\nu_t r\left(\frac{\partial V}{\partial z} + \frac{\partial U}{\partial r}\right)\right)$$
$$+\frac{8}{3}(U^2 + V^2)k - \frac{2\nu_t}{|U|}\left(U^2\frac{\partial U}{\partial z} + V^2\frac{\partial V}{\partial r} + UV\left(\frac{\partial U}{\partial r} + \frac{\partial V}{\partial z}\right)\right) \tag{9}$$

Model equation for dissipation rate (ε)

$$U\frac{\partial \varepsilon}{\partial z} + \frac{V}{r}\frac{\partial (r\varepsilon)}{\partial r} = \frac{\partial}{\partial z}\left(\left(\nu J + \frac{\nu_t}{\sigma_\varepsilon}\right)\frac{\partial \varepsilon}{\partial z}\right) + \frac{1}{r}\frac{\partial}{\partial r}\left(\left(\nu J + \frac{\nu_t}{\sigma_\varepsilon}\right)\frac{\partial \varepsilon}{\partial r}\right)$$
$$+C_{\varepsilon 1}\frac{\varepsilon}{k}P_k - C_{\varepsilon 2}\frac{\varepsilon^2}{k} - 2\phi\frac{\nu}{K}\varepsilon - 2\phi^2\frac{c_F}{K^{1/2}}\left(\frac{4}{3}|U|\varepsilon + \frac{1}{|U|}\left(C_{\varepsilon 3}\frac{k}{\varepsilon}\right.\right.$$
$$\left(\left(2\nu_t U\frac{\partial U}{\partial z} - \frac{2}{3}kU\right)\frac{\partial \varepsilon}{\partial z} + \left(2\nu_t V\frac{\partial V}{\partial r} - \frac{2}{3}kV\right)\frac{\partial \varepsilon}{\partial r} + U\nu_t\left(\frac{\partial U}{\partial r} + \frac{\partial V}{\partial z}\right)\frac{\partial \varepsilon}{\partial r}\right.$$
$$+V\nu_t\left(\frac{\partial V}{\partial z} + \frac{\partial U}{\partial r}\right)\frac{\partial \varepsilon}{\partial z}\right) + \frac{4}{3}\nu\frac{\partial |U|}{\partial z}\frac{\partial k}{\partial z} + \frac{4}{3}\nu\frac{\partial |U|}{\partial r}\frac{\partial k}{\partial r}$$
$$-\nu\left(\frac{\partial}{\partial z}\left(\frac{U^2}{|U|}\right)\frac{\partial}{\partial z}\left(\nu_t\frac{\partial U}{\partial z}\right) + \frac{\partial}{\partial r}\left(\frac{U^2}{|U|}\right)\frac{\partial}{\partial r}\left(\frac{\partial U}{\partial z}\right)\right. \tag{10}$$
$$+\frac{\partial}{\partial z}\left(\frac{UV}{|U|}\right)\frac{\partial}{\partial z}\left(\nu_t\left(\frac{\partial U}{\partial r} + \frac{\partial V}{\partial z}\right)\right) + \frac{\partial}{\partial r}\left(\frac{UV}{|U|}\right)\frac{\partial}{\partial r}\left(\nu_t\left(\frac{\partial U}{\partial r} + \frac{\partial V}{\partial z}\right)\right)$$
$$+\frac{\partial}{\partial z}\left(\frac{V^2}{|U|}\right)\frac{\partial}{\partial z}\left(\nu_t\frac{\partial V}{\partial r}\right) + \frac{\partial}{\partial r}\left(\frac{V^2}{|U|}\right)\frac{\partial}{\partial r}\left(\nu_t\frac{\partial V}{\partial r}\right)$$

C_μ, $C_{\varepsilon 1}$, $C_{\varepsilon 2}$, $C_{\varepsilon 3}$, C_s, σ_κ, σ_ε and σ_t are the constants used in the transport equations [8,9].

The boundary conditions are:
- Prescribed velocities, temperatures, turbulent kinetic energies and dissipation rates at the inlet.
- Velocity and turbulent kinetic energy are set equal to zero, and $\varepsilon = \nu \, \partial^2 k / \partial r^2$, at the walls.
- The outer cylinder is perfectly insulated.
- A wall function approach was used for treating the flow close to the wall [5].
- At the porous-clear fluid interface, the stress jump is described by an adjustable coefficient β which accounts for the stress jump at the interface, as in [10]:

$$(\mu + \mu_t)\frac{\partial U}{\partial r}\bigg|_f - (\mu_e + \mu_t)\frac{\partial U}{\partial r}\bigg|_p = (\mu + \mu_t)\frac{\beta}{\sqrt{K}}U\bigg|_{interface} \quad (11)$$

$$\left(\mu + \frac{\mu_t}{\sigma_k}\right)\frac{\partial k}{\partial r}\bigg|_f - (\mu_e + \frac{\mu_t}{\sigma_k})\frac{\partial k}{\partial r}\bigg|_p = (\mu + \mu_t)\frac{\beta}{\sqrt{K}}k\bigg|_{interface} \quad (12)$$

III. NUMERICAL DETAILS

A control volume approach is used to solve the model equations (1)-(10) with the specified boundary conditions. The well-established SIMPLE algorithm is followed for handling the pressure-velocity coupling. The governing equations are converted into a system of linear algebraic equations through integration over each control volume method. The algebraic equations are solved by using a line by line iterative method. The method sweeps the domain of integration along the r and z-axis and uses the tri-diagonal matrix inversion algorithm to solve the system of equations. After several trial computations to test the code sensitivity, a uniform zonal grid with different step sizes in each region (porous and fluid) is utilized. The convergence criterion is monitored in terms of the normalized residue of the algebraic equation. The maximum residue allowed for convergence check is set to 10^{-4} and the maximum absolute error on the heat flux transferred between the two fluids over the entire heat exchanger is less than 10^{-6}.

IV. RESULTS AND DISCUSSION

Computations are carried out for water flow in tubular heat exchanger of diameter ratio equal to 2. The effective viscosity in the porous medium equals the fluid viscosity (Brinkman assumption, J=1). The porosity of the porous material equals 0.95 and the inertia coefficient in the porous medium C_F is taken equal to 0.1.

For low thermal conductivity porous material ($R_c=1$) which can be used for insulation, Figure 2 exhibits the variation of the Nusselt number as function of the porous layer thickness (e) for different values of the Darcy number characterizing the permeability of the porous material (Da). As it shown in this figure, the heat transfer is improved for lower porous layer thickness and even passes the fluid case without porous medium (e=0). There exist optimal values of the Nusselt number that depend on the Darcy number. The more permeable is the medium, the higher is the heat transfer.
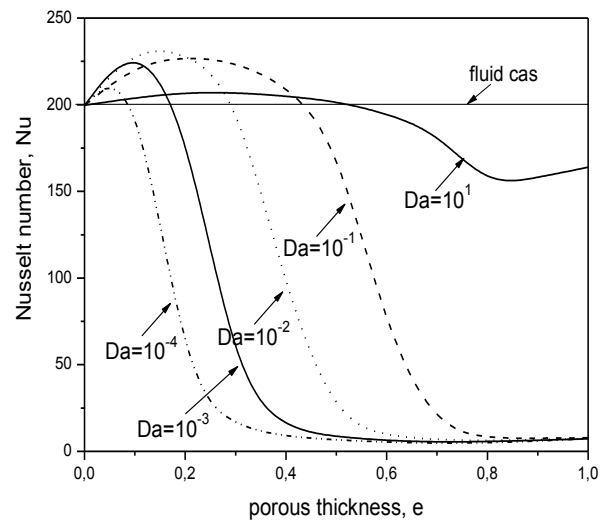

Fig. 2. Effect of porous layer thickness on Nusselt number for different values of Darcy number.

The effects of the porous layer thickness and the Darcy number on the rate of total entropy generation due to both heat transfer and dissipation are illustrated in Fig. 3. The entropy generation seems to be very sensitive to the porous layer thickness variation. There exist optimal and critical values of porous layer thicknesses of which minima and maxima entropy generation rate are obtained. These values depend greatly on permeability. This is due to the heat transfer and fluid flow irreversibility distribution in the annular heat exchanger. Also, we can notice that for weaker values of porous layer thickness where the heat transfer is enhanced, the total entropy generation is reduced.
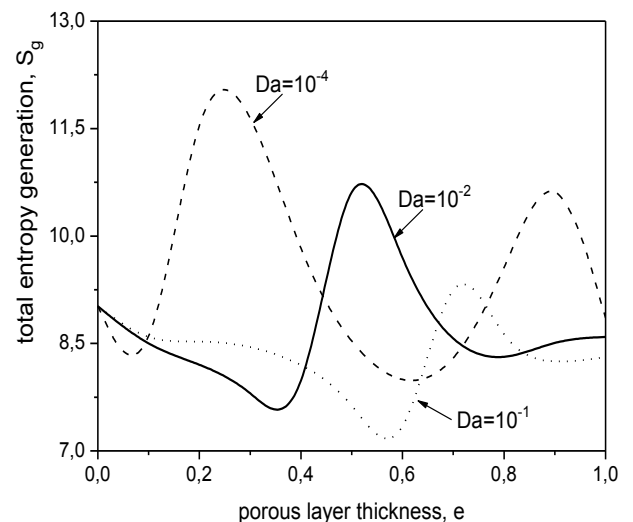

Fig. 3. Effect of porous layer thickness and Darcy number on the rate of total entropy generation ($R_c = 1$).

Considering now the case of porous medium with a higher thermal conductivity ($R_c > 1$) which in practical situation is more often to occur. The temperature of the cold fluid at the exit of the heat exchanger increases with the increase of the thermal conductivity ratio whatever the

porous layer thickness is. Moreover, there exists a critical value of the thermal conductivity ratio above which the cold fluid temperature is augmented and even passes the one of the fluid case without the porous substrate (Fig. 4). This critical value decreases when the permeability increases.
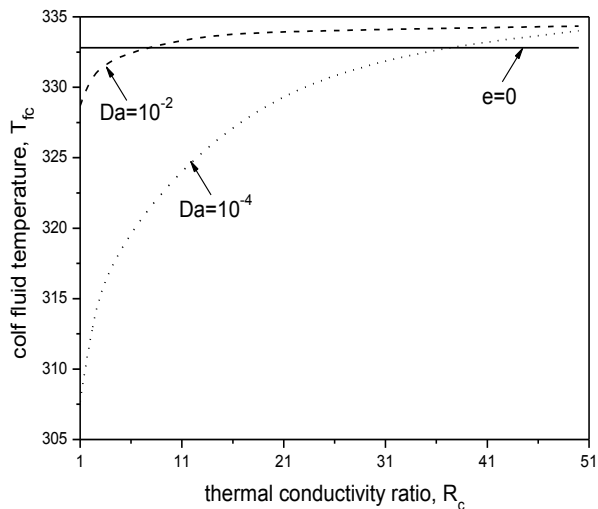

Fig. 4. Effect of thermal conductivity ratio on temperature of the cold fluid.

A substantial reduction of the rate of total entropy is obtained for lower values of porous layer thickness ($e \leq 40\%$) and when the porous substrate is a good thermal conductor. The effect of the thermal conductivity ratio is displayed in Fig. 5, for a given permeability ($Da = 10^{-2}$). We can notice that for the thin porous layers, there exists an optimal value corresponding to minimum entropy generation. This case is thermodynamically more advantageous.
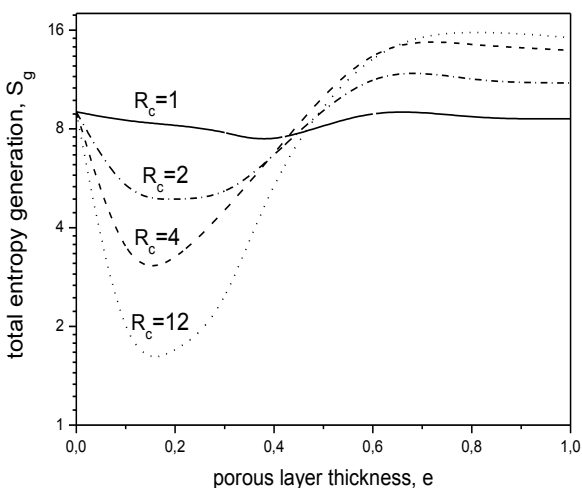

Fig. 5. Effect of thermal conductivity ratio on the rate of total entropy generation ($Da=10^{-2}$).

V. CONCLUSION

Computations for turbulent flow with the modified κ-ε model and the entropy generation equation that accounts for the turbulent stress, in annular heat exchanger partially or totally filled with porous material were performed. The numerical predictions based on the finite volume method show that for a given Darcy number and lower values of porous layer thickness, an increase in the thermal conductivity ratio leads to an improvement of the heat transfer and minimization of the rate of total entropy generation.

TABLE I
NOMENCLATURE

Symbol	Quantity	Units
C_p	specific heat of fluid	J/(kg.K)
c_F	Forchheimer inertia coefficient	-
D_h	hydraulic diameter	m
Da	Darcy number	-
e	porous layer thickness	m
J	viscosity ratio	-
k	turbulent kinetic energy	m^2/s^2
K	Permeability	m^2
Nu	Nusselt number	-
P	pressure	Pa
Pr	Prandtl number	-
r	radial direction	-
R_c	conductivity ratio	-
$\dot{S}$	entropy generation rate per volume unit	W/(m^3.K)
S	entropy generation rate	W/K
$\overline{T}$	time averaged temperature	K
U	axial time-averaged fluid velocity	m/s
V	radial time-averaged fluid velocity	m/s
z	axial direction	-
λ	thermal conductivity	W/(m^2.K)
ρ	density	kg/m^3
μ	dynamic viscosity	kg/(m.s)
ν	kinematic viscosity	m^2/s
ε	dissipation rate	-
ϕ	Porosity	-

Subscript	
c	cold
e	effective
f	fluid
h	hot
in	inlet
g	total
p	porous
t	turbulent

REFERENCES

[1] Y. Demirel and R. Kahraman, "Entropy Generation in Rectangular Packed Duct with Wall Heat Flux," *Int. J. of Heat and Mass Transfer*, vol. 42, pp. 2337-2344, 1999.

[2] T. V. Morosuk. "Entropy Generation in Conduits Filled with Porous Medium Totally and Partially," *Int. J. of Heat and Mass Transfer*, vol. 48, pp. 2548-2560, 2005.

[3] N. Allouache and S. Chikh. "Second Law Analysis in a Partly Porous Double Pipe Heat Exchanger," *ASME, Journal of Applied Mechanics*, vol. 73, pp. 60-65, 2006.

[4] D. Getachew, W. J. Minkowycz and J. L. Lage, "A modified form of the model for turbulent flows of an incompressible fluid in porous media," *Int. J. Heat Mass Transfer*, vol. 43, pp. 2909-2915, 2000.

[5] N. Allouache and S. Chikh. "Numerical modeling of turbulent flow in an annular heat exchanger partly filled with a porous substrate," *Journal of Porous Media*, vol. 7, pp. 617-632, 2008.

[6] F. Kock and H. Herwig. "Entropy Production Calculation for Turbulent Shear Flows and their Implementation in CFD Codes," *Int. J. of Heat and Fluid Flow*, vol. 26, pp. 672-680, 2005.

[7] H. Herwig and F. Kock, "Direct and indirect methods of calculating entropy generation rates in turbulent convective heat transfer problems", *Heat Mass Transfer*, vol. 43, pp. 207-215, 2007.

[8] G. L. Mellor and H. J. Herring, 1973, "A survey of mean turbulent field closure models", *A/AA Jl*, vol. 11, pp. 590-599, 1973.

[9]   B. E. Launder, B. E, and D. B. Spalding, , "The numerical computation of turbulent flow", *Comput. Meth. Appl. Mech. Eng*., vol. 3, pp. 269-289, 1974.

[10] R. A. Silva and M. J. S. de Lemos, "Turbulent flow in a channel occupied by a porous layer considering the stress jump at the interface," *Int. J. of Heat and Mass Transfer*, vol. 46, pp. 5113-5121, 2003.